Available online at www.sciencedirect.com
SCIENCE DIRECT®
International Journal of Heat and Fluid Flow 26 (2005) 817–825
International Journal of HEAT AND FLUID FLOW
www.elsevier.com/locate/ijhff

Dynamic behaviour of high-pressure natural-gas flow in pipelines

L.M.C. Gato *, J.C.C. Henriques [1]

Department of Mechanical Engineering, Instituto Superior Técnico, Technical University of Lisbon, Av. Rovisco Pais, 1049-001 Lisboa, Portugal

Received 3 January 2004; received in revised form 18 January 2005; accepted 2 March 2005
Available online 4 June 2005

Abstract

The aim of the present study is the numerical modelling of the dynamic behaviour of high-pressure natural-gas flow in pipelines. The numerical simulation was performed by solving the conservation equations, for one-dimensional compressible flow, using the Runge–Kutta discontinuous Galerkin method, with third-order approximation in space and time. The boundary conditions were imposed using a new weak formulation based on the characteristic variables. The occurrence of pressure oscillations in natural-gas pipelines was studied as a result of the compression wave originated by the rapid closure of downstream shut-off valves. The effect of the partial reflection of pressure waves was also analyzed in the transition between pipes of different cross-sectional areas.

Keywords: Unsteady compressible flow; Gas pipelines; Gas transients; Discontinuous Galerkin method

1. Introduction

In the analysis of unsteady flow in gas pipelines we observe the occurrence of rapid and slow disturbances. In general, slow disturbances are originated by pressure and mass-flow fluctuations as a result of the cyclic variation in the gas demand along the day. These disturbances are associated with the compression and expansion of the gas in the pipeline and they are usually studied with simplified computational models, which neglect the variation of the fluid kinetic energy (ignoring the convection term in the momentum equation) (Thorley and Tiley, 1987). Rapid disturbances are associated with wave effects caused by events such as the sharp closure of a shut-off valve, the system startup or the pipeline rupture.

Numerical simulation of fast transients have been performed by using the method of characteristics (Rao and Eswaran, 1993, Kessal, 2000), the finite difference (Thorley and Tiley, 1987) and the finite volume methods (Greyvenstein, 2002; Osiadacz and Chaczykowski, 2001) and, more recently, the total variation diminishing (TVD) finite volume method (Zhou and Adewumi, 2000; Ibraheem and Adewumi, 1999). The accuracy of the above methods was restricted to second-order.

High-order methods can provide a way to significantly improve the accuracy of the numerical solution of rapid transient flow in gas pipelines due to their ability to capture strong gradients of the exact solution without producing spurious oscillations. Comprehensive reviews of high-order accurate methods for the numerical solution of compressible fluid flow are presented in Abgrall et al. (1999), Cockburn (1999) and Shu (1999). The Runge–Kutta discontinuous Galerkin (RKDG) method has an important advantage over other high-order methods: the discontinuous Galerkin space-discretization permits simple generalization of the degree of approximation to *n*th-order, since no

* Corresponding author. Tel.: +351 21 841 7411; fax: +351 21 841 7398.
E-mail addresses: lgato@mail.ist.utl.pt (L.M.C. Gato), jcch@mail.ist.utl.pt (J.C.C. Henriques).
[1] Partially supported by IDMEC/IST.

0142-727X/$ - see front matter © 2005 Elsevier Inc. All rights reserved.
doi:10.1016/j.ijheatfluidflow.2005.03.011

Nomenclature

Roman symbols

a	$(\gamma p/\varrho)^{\frac{1}{2}}$, speed of sound
A	cross-sectional area
$\mathbf{A}$	flux Jacobian, Eq. (6)
C_p	specific heat at constant pressure
C_v	specific heat at constant volume
E	specific stagnation energy
$\mathbf{F}$	flux vector, Eq. (3)
H	$E + p/\varrho$, specific stagnation enthalpy
$\mathbf{H}$	flux function, Eq. (8)
$\mathbf{L}$	left set of eigenvectors of $\mathbf{A}$
$\mathbf{L}_h$	time derivative of $\mathbf{U}_h$, Eq. (11)
p	static pressure
p_0	stagnation pressure
$P_i(x)$	Legendre polynomial of degree i
PRV	pressure regulator valve
$\partial\mathbf{Q}$	auxiliary variables
R	gas constant
$\mathbf{R}$	right set of eigenvectors of $\mathbf{A}$
$\mathbf{S}$	source term, Eq. (3)
t	time
T	absolute temperature
TSV	turbine shut-off valves
$\partial\mathbf{U}$	conservative variables, Eq. (2)
u	flow velocity
v_h	discrete test functions
$\partial\mathbf{V}$	primitive variables
$\partial\mathbf{W}$	characteristic variables, Eq. (16)
x	distance along pipeline
Z	compressibility factor

Greeks

γ	C_p/C_v, specific heats ratio
Δ	variation
μ	viscosity
$\mathbf{\Lambda}$	set of eigenvalues of $\mathbf{A}$
Ω	computational domain
τ_w	wall shear stress
θ	integration parameter
ϱ	density

Subscripts

in	inlet values
h	approximate solution
j	element number
max	maximum value
N	number of elements
out	outlet values

Superscripts

$-$	left state
$+$	right state
i	vector component
k	degree of the approximate solution
n	time step

special treatment of the boundary conditions is required to achieve uniform high-order accuracy (Cockburn, 1999).

In this paper, we consider gradually varying cross-sectional area along the duct and the effect of fluid friction in the flow model to study the occurrence of rapid disturbances in high-pressure natural-gas flow in pipelines, using a high-order RKDG method, developed at Instituto Superior Técnico, for the calculation of rapid transients in gas pipelines. The boundary conditions are imposed using a new characteristic formulation, which allows the accurate simulation of the transient flow conditions, as a result of the sharp closure of valves in pipelines, as well as the steady-state initial conditions.

The mathematical model considers the following assumptions: the flow is compressible and one-dimensional; the flow includes rapid transients; the flow is adiabatic (consistent with the previous assumption); the fluid entropy may vary as function of the pipe length, x, and the time, t; variations in potential energy may be ignored; the viscous effects are modelled by considering the pipeline-wall shear stress; the pipeline cross-sectional area is a function of x only (rigid wall), within the limitations consistent with one-dimensional flow; the heat diffusion in the fluid is neglected.

2. Equations for one-dimensional compressible flow

We consider an element of volume $A(x)\mathrm{d}x$, where $A(x)$ is the cross-sectional area of the duct. In an inertial frame of reference, the equations describing one-dimensional adiabatic compressible gas flow can be written in the so-called conservative form

$$\partial_t \mathbf{U} + \partial_x \mathbf{F} = \mathbf{S}, \tag{1}$$

with $x \in [0, L]$ and $t \in [0, \mathscr{T}]$. The vector of conservative variables, $\mathbf{U}$, the flux vector, $\mathbf{F}$, and the source term, $\mathbf{S}$, associated with the area change and the effect of fluid friction, are given by

$$\mathbf{U} = \begin{pmatrix} U_0 \\ U_1 \\ U_2 \end{pmatrix} = \begin{pmatrix} \varrho A \\ \varrho u A \\ \varrho E A \end{pmatrix}, \tag{2}$$

$$\mathbf{F} = \begin{pmatrix} F_0 \\ F_1 \\ F_2 \end{pmatrix} = \begin{pmatrix} \varrho u A \\ \varrho u^2 A + pA \\ \varrho u H A \end{pmatrix},$$
$$\mathbf{S} = \begin{pmatrix} S_0 \\ S_1 \\ S_2 \end{pmatrix} = \begin{pmatrix} 0 \\ p d_x A - \tau_w \pi D \\ 0 \end{pmatrix}. \tag{3}$$

The system of equations (1) is subject to suitable initial conditions $\mathbf{U}^0(x) = \mathbf{U}(x,0)$, and to boundary conditions $\mathbf{U}_0(t) = \mathbf{U}(0,t)$ and $\mathbf{U}_L(t) = \mathbf{U}(L,t)$ (to be introduced in Section 4). The variables of the system are: the density, ϱ; the flow velocity, u; the pressure, p; the specific total energy, E; and the specific total enthalpy, $H = E + p/\varrho$. The first equation is known as the equation of continuity and states the conservation of mass. The second equation results from the momentum conservation. The third equation expresses the conservation of energy within the control volume. To close the system, we use the equation of state $p = Z\varrho RT$, where R is the gas constant and Z is the compressibility factor ($Z = 1$ for a perfect gas). This equation introduces an additional variable, the temperature of the fluid, T. If we assume that the compressibility factor, Z, and the specific heat at constant pressure, C_p, are constant, in the range of the pressure and the temperature of the flow, we get the following relationships $E = C_v T + u^2/2$, $H = C_p T + u^2/2$ and $ZR = C_p - C_v$ that close the system. Therefore, the pressure can be written as $p = (\gamma - 1)(\varrho E - \varrho u^2/2)$, where $\gamma = C_p/C_v$.

3. The Runge–Kutta discontinuous Galerkin method

3.1. Weak formulation

Let us split the computational domain $\Omega = [0, L]$ in N equally spaced finite elements, $I_j = (x_{j-1/2}, x_{j+1/2})$, with length $\Delta x = L/N$. We seek an approximate solution $\mathbf{U}_h$ of $\mathbf{U}$ such that, for a given time instant $t \in [0, T]$, $\mathbf{U}_h(t)$ belongs to a finite dimensional space $V_h = V_h^k \equiv \{v \in L^2(0,L) : v|_{I_j} \in P^k(I_j),\ j = 1, \ldots, N\}$, where $P^k(I_j)$ is the space of the polynomials in I_j of degree at most k. To find the approximate solution $\mathbf{U}_h$, let us use a weak formulation as follows. We begin by multiplying each equation i of the system (1) by an arbitrary smooth function v, and then integrate in I_j. Afterwards, we integrate by parts and get (Cockburn and Shu, 1989)

$$\int_{I_j} \partial_t U_{h_i}(x,t) v_h(x) \mathrm{d}x - \int_{I_j} F_i(\mathbf{U}_h(x,t)) \partial_x v_h(x) \mathrm{d}x + H_i(\mathbf{U}_h(x_{j+1/2},t)) v_h(x_{j+1/2}^-) - H_i(\mathbf{U}_h(x_{j-1/2},t)) v_h(x_{j-1/2}^+) = \int_{I_j} S_i v(x) \mathrm{d}x, \tag{4}$$

where the functions v were replaced by discrete test functions v_h, belonging to the space V_h, the exact solution $\mathbf{U}$ by the approximate solution $\mathbf{U}_h$, and the non-linear flux, $\mathbf{F}(\mathbf{U}(x_{j+1/2}, t))$, by a numerical flux function

$$\mathbf{H}(\mathbf{U}_h(x_{j+1/2},t)) = \begin{pmatrix} H_0 \\ H_1 \\ H_2 \end{pmatrix} = \mathbf{H}\left(\mathbf{U}\left(x_{j+1/2}^-, t\right), \mathbf{U}\left(x_{j+1/2}^+, t\right)\right) \tag{5}$$

to be defined later.

3.2. Energy stable flux function

The system of equations (1) may be written in the quasi-linear form

$$\partial_t \mathbf{U} + \mathbf{A} \partial_x \mathbf{U} = \mathbf{S}, \tag{6}$$

with

$$\mathbf{A} = \frac{\partial \mathbf{F}}{\partial \mathbf{U}} = \begin{pmatrix} 0 & 1 & 0 \\ \frac{1}{2}u^2(\gamma - 3) & -u(\gamma - 3) & \gamma - 1 \\ u^3(\gamma - 1) - \gamma u E & -\frac{3}{2}u^2(\gamma - 1) + \gamma E & \gamma u \end{pmatrix}. \tag{7}$$

The matrix $\mathbf{A}$ can be decomposed by means of a similarity transformation $\mathbf{A} = \mathbf{R}\boldsymbol{\Lambda}\mathbf{L}$, where $\mathbf{R} = \mathbf{L}^{-1}$ and $\boldsymbol{\Lambda}$ are, respectively, the matrices of the right set of eigenvectors and the set of eigenvalues (see Hirsch, 1990 for details).

Given two states $\mathbf{U}_{j+1/2}^- = \mathbf{U}(x_{j+1/2}^-)$ and $\mathbf{U}_{j+1/2}^+ = \mathbf{U}(x_{j+1/2}^+)$, a stable energy-flux function, for the Riemann problem, is given by (Barth, 1999, Barth and Charrier, 2001)

$$\mathbf{H}_{j+1/2} = \frac{1}{2}\left(\mathbf{F}_{j+1/2}^+ + \mathbf{F}_{j+1/2}^- - |\bar{\mathbf{A}}|\left(\mathbf{U}_{j+1/2}^+ - \mathbf{U}_{j+1/2}^-\right)\right), \tag{8}$$

with

$$|\bar{\mathbf{A}}| = \frac{1}{2}\int_{-1}^{1} |\mathbf{A}(\bar{\mathbf{U}}(\theta))| \mathrm{d}\theta, \tag{9}$$

where (9) is defined in the usual matrix sense via eigensystem decomposition $|\mathbf{A}| = \mathbf{R}|\boldsymbol{\Lambda}|\mathbf{L}$ and $\bar{\mathbf{U}}(\theta) = (1-\theta)\mathbf{U}_{j+1/2}^-/2 + (1+\theta)\mathbf{U}_{j+1/2}^+/2$. Barth (1999) has shown that the matrix (9) can be evaluated using a Gauss–Legendre quadrature with p points.

3.3. System of equations and time integration

Following Cockburn (1999), we choose the Legendre polynomials, $P_i(x)$, as local shape functions. The approximate solution of kth-order order is then given by

$$U_{h_i}(x,t) = \sum_{m=0}^{k} U_{h_i}^m(t) P_m(x). \tag{10}$$

Replacing (10) in (4), we obtain a diagonal system of linear equations with $k+1$ unknowns per element I_j,

$$\partial_t \mathbf{U}_h = \mathbf{L}_h, \tag{11}$$

to be determined at each time-step.

To discretize the system of differential equations (11) in time, we use an explicit third-order total variation diminishing (TVD) Runge–Kutta scheme (Cockburn, 1999),

$$\begin{aligned}
\mathbf{U}_h^{(1)} &= \mathbf{U}_h^n + \Delta t \mathbf{L}_h\left(\mathbf{U}_h^n\right),\\
\mathbf{U}_h^{(2)} &= \frac{3}{4}\mathbf{U}_h^n + \frac{1}{4}\mathbf{U}_h^{(1)} + \frac{1}{4}\Delta t \mathbf{L}_h\left(\mathbf{U}_h^{(1)}\right),\\
\mathbf{U}_h^{n+1} &= \frac{1}{3}\mathbf{U}_h^n + \frac{2}{3}\mathbf{U}_h^{(2)} + \frac{2}{3}\Delta t \mathbf{L}_h\left(\mathbf{U}_h^{(2)}\right),
\end{aligned} \tag{12}$$

under the stability condition $\Delta t \leqslant \Delta x f_1 \Lambda_{\max}^{-1}$. Cockburn and Shu (1989) suggest $f_1 = (2k+1)^{-1}$. All the integrals that appear in the system of equations (11) are evaluated numerically using a Gauss–Legendre quadrature with p points (Cockburn, 1999).

4. Boundary conditions

The Runge–Kutta discontinuous Galerkin method allows a simple implementation of the boundary conditions when they are imposed through flux functions

$$\mathbf{H}(\mathbf{U})_{1/2}(t) = \mathbf{H}\left(\mathbf{U}_{\text{in}}(t), \mathbf{U}\left(x_{1/2}^+, t\right)\right) \tag{13}$$

and

$$\mathbf{H}(\mathbf{U})_{N+1/2}(t) = \mathbf{H}\left(\mathbf{U}\left(x_{N+1/2}^-, t\right), \mathbf{U}_{\text{out}}(t)\right), \tag{14}$$

at the inlet, $x_{1/2}^-$, and outlet, $x_{N+1/2}^+$, sections. The states $\mathbf{U}_{\text{in}}(t)$ and $\mathbf{U}_{\text{out}}(t)$ are evaluated according to the prescribed boundary condition.

The system of equations (1) can be written in the characteristic form, $\partial_t \mathbf{W} + \mathbf{\Lambda}\partial_x \mathbf{W} = \widetilde{\mathbf{S}}$, with $\partial\mathbf{W} = \mathbf{L}\partial\mathbf{U}$ and $\widetilde{\mathbf{S}} = \mathbf{L}\mathbf{S}$. We select well-posed boundary conditions by prescribing the characteristic variables whose convection velocity direction is towards the interior of the domain at the boundary. In this way, the number of boundary conditions is a function of the signs of the eigenvalues of $\mathbf{\Lambda}$.

The boundary conditions are simpler to implement if we consider the set of primitive variables, $\mathbf{V} = (\varrho A \; uA \; pA)^{\mathrm{T}}$, which are related to the set of conservative variables by

$$\frac{\partial \mathbf{U}}{\partial \mathbf{V}} = \begin{pmatrix} 1 & 0 & 0 \\ u & \varrho & 0 \\ \frac{1}{2}u^2 & \varrho u & \frac{1}{\gamma-1} \end{pmatrix}. \tag{15}$$

The characteristic variables, written as functions of the primitive variables, take the form

$$\partial\mathbf{W} = \begin{pmatrix} \partial W_1 \\ \partial W_2 \\ \partial W_3 \end{pmatrix} = \frac{\partial \mathbf{W}}{\partial \mathbf{V}}\partial\mathbf{V} = \begin{pmatrix} \partial(\varrho A) - a^{-2}\partial(pA) \\ \partial(uA) + (\varrho a)^{-1}\partial(pA) \\ \partial(uA) - (\varrho a)^{-1}\partial(pA) \end{pmatrix}, \tag{16}$$

where the Jacobian matrix of the transformation is given by

$$\frac{\partial \mathbf{W}}{\partial \mathbf{V}} = \begin{pmatrix} \mathbf{l}_1 \\ \mathbf{l}_2 \\ \mathbf{l}_3 \end{pmatrix} = \begin{pmatrix} 1 & 0 & -a^{-2} \\ 0 & 1 & (\varrho a)^{-1} \\ 0 & 1 & -(\varrho a)^{-1} \end{pmatrix}. \tag{17}$$

4.1. Initial conditions for transient flow

The initial conditions for transient flow are given by the steady-state flow solution, for prescribed inlet and outlet conditions. This steady-state solution is obtained by running the solver that implements the above formulation, starting from an arbitrary physically consistent initial condition and imposing the following steady-state boundary conditions, until the desired degree of convergence is achieved.

4.1.1. Inlet boundary conditions for steady-state

The inlet boundary conditions for steady-state consist in imposing the stagnation specific enthalpy, H, and the stagnation pressure, p_0, defined as

$$p_0 A = pA\left(1 + \frac{1}{2}(\gamma-1)\frac{u^2}{a^2}\right)^{\gamma(\gamma-1)^{-1}}. \tag{18}$$

The third equation is determined from the characteristic property that is convected outwards with respect to the domain, ∂W_3, resulting in an inlet state given by

$$\mathbf{U}_{\text{in}}(t) = \mathbf{U}(x_{1/2}^+, t) + \left.\frac{\partial \mathbf{U}}{\partial \mathbf{V}}\frac{\partial \mathbf{V}}{\partial \mathbf{Q}}\right|_{\text{in}} \Delta\mathbf{Q}_{\text{in}}, \tag{19}$$

with

$$\partial\mathbf{Q}_{\text{in}} = (\partial(HA) \quad \partial(p_0 A) \quad \partial W_3)^{\mathrm{T}}, \tag{20}$$

$$\left.\frac{\partial \mathbf{Q}}{\partial \mathbf{V}}\right|_{\text{in}} = \left(\left.\frac{\partial \mathbf{V}}{\partial \mathbf{Q}}\right|_{\text{in}}\right)^{-1} = \begin{pmatrix} \frac{\partial(HA)}{\partial(\varrho A)} & \frac{\partial(HA)}{\partial(uA)} & \frac{\partial(HA)}{\partial(pA)} \\ \frac{\partial(p_0 A)}{\partial(\varrho A)} & \frac{\partial(p_0 A)}{\partial(uA)} & \frac{\partial(p_0 A)}{\partial(pA)} \\ 0 & 1 & -(\varrho a)^{-1} \end{pmatrix}, \tag{21}$$

and

$$\Delta\mathbf{Q}_{\text{in}} = \begin{pmatrix} (HA)_{\text{in}} - (HA)(x_{1/2}^+, t) \\ (p_0 A)_{\text{in}} - (p_0 A)(x_{1/2}^+, t) \\ 0 \end{pmatrix}. \tag{22}$$

The third row of the Jacobian matrix (21) is taken from the third row, $\mathbf{l}_3$, of the matrix (17). The derivatives that

appear in the Jacobian matrix (21) are evaluated analytically.

4.1.2. Outlet boundary conditions for steady-state

As outlet boundary condition we impose the mass flow, $(\varrho uA)_s$. The other two boundary conditions to be imposed are the characteristic variables that are convected towards the exterior of the domain, ∂W_2 and ∂W_3, from which we obtain

$$\mathbf{U}_s(t) = \mathbf{U}(x^-_{N+1/2}, t) + \left.\frac{\partial \mathbf{U}}{\partial \mathbf{Q}}\right|_{\text{out}} \Delta\mathbf{Q}_{\text{out}}, \tag{23}$$

with $\partial\mathbf{Q}_{\text{out}} = (\partial(\varrho uA)\ \partial W_2\ \partial W_3)^{\mathrm{T}}$, and

$$\Delta\mathbf{Q}_{\text{out}} = \begin{pmatrix} (\varrho uA)_{\text{out}} - (\varrho uA)(x^-_{N+1/2}, t) & 0 & 0 \end{pmatrix}^{\mathrm{T}}. \tag{24}$$

The Jacobian matrix, $(\partial\mathbf{U}/\partial\mathbf{Q}_{\text{out}})$, is determined in an analogous way to the previous case.

4.2. Transient flow

4.2.1. Inlet boundary conditions for opened gas-pressure regulators

For opened gas-pressure regulators in transient flow, as inlet boundary conditions we impose $(p\varrho^{-1})_{\text{in}}(t)$ (which is proportional to the static temperature T) and the mass flow, $(\varrho uA)_{\text{in}}(t)$, as functions of the time. The third equation is given by the third characteristic, giving

$$\mathbf{U}_{\text{in}}(t) = \mathbf{U}(x^+_{1/2}, t) + \left.\frac{\partial \mathbf{U}}{\partial \mathbf{Q}}\right|_{\text{in}} \Delta\mathbf{Q}_{\text{in}}, \tag{25}$$

with $\partial\mathbf{Q}_{\text{in}} = (\partial(p\varrho_{-1})\ \partial(\varrho u A)\ \partial W_3)^{\mathrm{T}}$, and

$$\Delta\mathbf{Q}_{\text{in}} = \begin{pmatrix} (p\varrho^{-1})_{\text{in}}(t) - (p\varrho^{-1})(x^+_{1/2}, t) \\ (\varrho uA)_{\text{in}}(t) - (\varrho uA)(x^+_{1/2}, t) \\ 0 \end{pmatrix}. \tag{26}$$

4.2.2. Inlet boundary condition for closed gas-pressure regulators

When the gas-pressure regulator is closed, the boundary condition is similar to a solid wall condition, $(\varrho uA)_{\text{in}}(t) = 0$, resulting in

$$\mathbf{U}_{\text{in}}(t) = \mathbf{U}\left(x^+_{1/2}, t\right) + \left.\frac{\partial \mathbf{U}}{\partial \mathbf{Q}}\right|_{\text{in}} \Delta\mathbf{Q}_{\text{in}}, \tag{27}$$

with $\partial\mathbf{Q}_{\text{in}} = (\partial(\varrho uA)\ \partial W_2\ \partial W_3)^{\mathrm{T}}$, and

$$\Delta\mathbf{Q}_{\text{in}} = \begin{pmatrix} -(\varrho uA)\left(x^+_{1/2}, t\right) & 0 & 0 \end{pmatrix}^{\mathrm{T}}. \tag{28}$$

4.2.3. Outlet boundary condition for opened shut-off valve

The boundary condition for an opened shut-off valve is equivalent to the boundary condition (23), with the mass flow changing in time

$$\Delta\mathbf{Q}_{\text{out}} = \begin{pmatrix} (\varrho uA)_{\text{out}}(t) - (\varrho uA)\left(x^-_{N+1/2}, t\right) & 0 & 0 \end{pmatrix}^{\mathrm{T}}. \tag{29}$$

4.2.4. Outlet boundary condition for closed shut-off valve

The outlet boundary condition for a closed shut-off valve is imposed in an analogous way to the previous boundary condition, considering zero mass flow.

5. Results

To illustrate the dynamic behaviour of high-pressure gas flow in pipelines, typical flow conditions were considered for a natural-gas supply pipeline, between the pressure-reducing (and metering) station and the emergency shut-off valves, upstream of a combined-cycle power-plant with three turbine-generator sets, with an installed capacity of 3×400 MW. In the design of this type of supply line, one key aspect is the dynamic behaviour of the system in the event of a sudden (emergency) shut-off of one or more valves of the turbine-generator sets. In this case, the pressure in the supply pipeline may reach excessive values and trigger the protective shut-off valves of the pressure-regulator station. To avoid this occurrence, it is necessary to conciliate the dynamic characteristics of the pressure regulator and the shut-off valves with the gas velocity, the volume and the length of the pipeline. As initial conditions, we assume a mass flow $\dot{m}_{\text{initial}} = 52.8$ kg/s (225,000 m^3(n)/h), a static temperature $T = 15$ °C and an absolute pressure $p = 33$ bar, at the exit of the pressure regulator valve. Properties of the natural gas used in the calculations are presented in Table 1.

Two parameters were used to characterize the dynamic response of the valves: the reaction time (time taken to start the valve actuation after sensing a pressure perturbation) and the actuation time (time interval between the initial and the final positions of the valve). For the shut-off valves we considered the actuation time only. In any case, linear variation of the mass-flow was assumed during the valve transient.

Six examples were considered including two pipeline lengths, $L = 350$ m (cases 1–4) and $L = 1600$ m (cases 5 and 6), typical (cases 1, 2, 5 and 6) and high-speed (cases 3 and 4) dynamic characteristics for the pressure-regulator and the shut-off valves, and total (cases 1–5) and partial (case 6) closure conditions for the shut-off valves. For simulation purposes, the pipelines were split into three elements, of different length and diameter, whose geometries are described in Table 2. Excluding case 2, the pipeline element diameters were selected to provide

Table 1
Gas properties in working conditions, $p = 33$ bar and $T = 15$ °C

R	440.7	m^2/(s^2 K)
Z	0.934	–
γ	1.417	–
μ	1.182×10^{-5}	kg/(m s)

Table 2
Pipeline geometry: L_i, length of element i; D_i, diameter of element i

Case	L_1 [m]	L_2 [m]	L_3 [m]	D_1 [m]	D_2 [m]	D_3 [m]
1	100	150	100	0.400	0.400	0.400
2	100	150	100	0.400	1.000	0.400
3	100	150	100	0.400	0.400	0.400
4	170	10	170	0.400	0.949	0.400
5	100	1200	300	0.300	0.500	0.400
6	100	1200	300	0.300	0.500	0.400

gas flow velocities within the typical range, for this type of flow, in steady-state conditions, between 10 and 30 m/s. A linear variation of the area along 4 m of duct length was assumed for the transition between elements with different cross-sectional areas.

Numerical results were obtained with third-order accuracy in time and space using second degree local basis functions and the TVD Runge–Kutta scheme (Eq. (12)). Figs. 1–4 show plots of the numerically obtained results for the mass-flow and the pressure distribution, as functions of time, for two sections at the exit of the pressure regulator valve (PRV) and immediately upstream of the emergency turbine shut-off valves (TSV). Case 1 refers to a supply line consisting of a single constant diameter pipeline, $D = 0.4$ m, and length $L = 350$ m, equipped with pressure regulator and shut-off valves, with dynamic characteristics typical of those normally found for valves of that size (Table 3). The calculation assumes the most severe condition of simultaneous closure of the three turbine shut-off valves. A pressure-wave front propagating towards the pressure regulator valve is generated just after the valves closure, keeping behind it a pressure increase of 1.7 bar, for $t = 0.25$ s, Figs. 1 and 2. For the considered pipeline length, the wave pressure reaches the pressure regulator valve after 0.85 s. The numerical results clearly show the interaction of the pressure wave, generated by the rapid closure of the turbine emergency shut-off valves, with the pressure regulator valve. The value for the maximum pressure predicted at the exit of the pressure regulator valve is 44.2 bar, which is reached 9.3 s after the valve closure. In the above example, the increase in mass in the system, due to the delay in the pressure regulator valve actuation relative to the turbine shut-off valves closure, originates a pressure increase much higher than that due to the pressure wave produced by the rapid

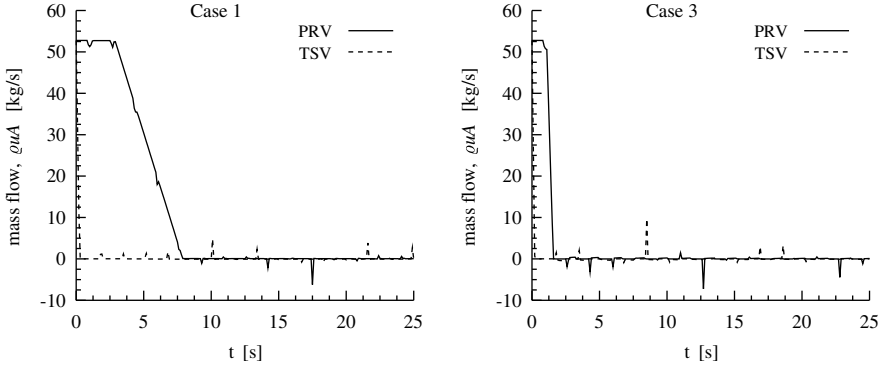

Fig. 1. Mass flow-rate downstream of the pressure regulator valve (PRV) and upstream of the emergency turbine shut-off valves (TSV), as function of time, for cases 1 and 3.

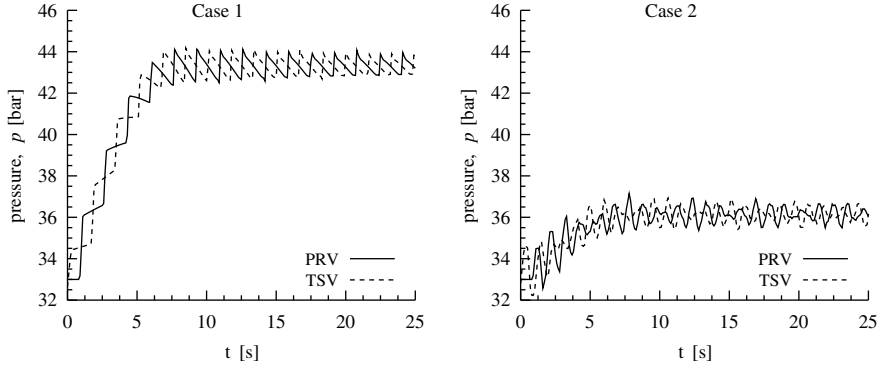

Fig. 2. Pressure distribution downstream of the pressure regulator valve (PRV) and upstream of the emergency turbine shut-off valves (TSV), as function of time, for cases 1 and 2.

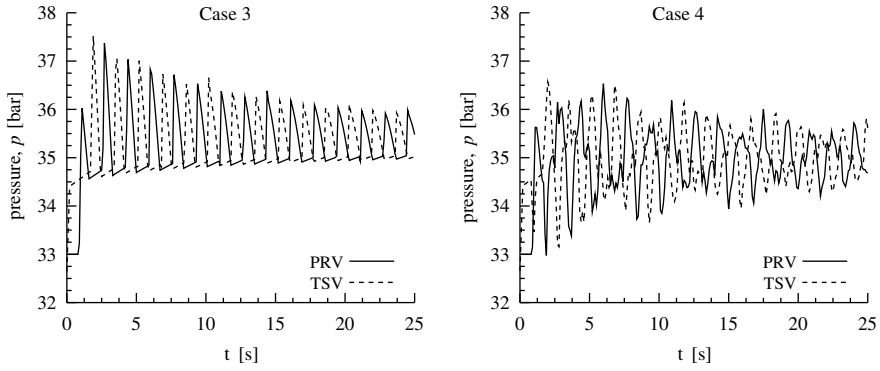

Fig. 3. Pressure distribution downstream of the pressure regulator valve (PRV) and upstream of the emergency turbine shut-off valves (TSV), as function of time, for cases 3 and 4.

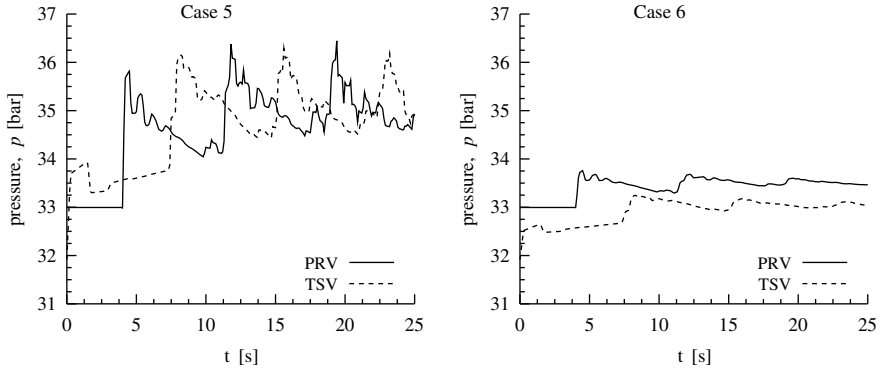

Fig. 4. Pressure distribution downstream of the pressure regulator valve (PRV) and upstream of the emergency turbine shut-off valves (TSV), as function of time, for cases 5 and 6.

Table 3
Boundary conditions: $\dot{m}_{\text{initial}}$, initial mass flow rate; $\dot{m}_{\text{final}}$, final mass flow rate; t_{reaction}, pressure regulator reaction time; $t_{\text{actuation}}$, pressure regulator actuation time; $t_{\text{shut-off}}$, shut-off valve closure time

Case	$\dot{m}_{\text{initial}}$ [m^3(n)/h]	$\dot{m}_{\text{final}}$ [m^3(n)/h]	t_{reaction} [s]	$t_{\text{actuation}}$ [s]	$t_{\text{shut-off}}$ [s]
1	225,000	0	2.00	5.00	0.25
2	225,000	0	2.00	5.00	0.25
3	225,000	0	0.20	0.50	0.20
4	225,000	0	0.20	0.50	0.20
5	225,000	0	2.00	5.00	0.25
6	225,000	150,000	2.00	5.00	0.25

closure of the turbine shut-off valves. This over-pressure, by mass accumulation, may be largely reduced by an appropriate increase in the pipeline volume, as shown by the numerically obtained results for case 2, Fig. 2, where an intermediate 150 m element of the original pipeline was replaced by a 1.0 m diameter element of the same length, keeping all the remaining conditions. In this case, the transition between pipes of different cross-sectional areas introduce partial wave reflections that combine with the pressure oscillations due to the closure of the valves, giving an irregular wave pressure distribution, Fig. 2. Mass-flow fluctuations shown in the graphs of Fig. 1, for cases 1 and 2, result from the use of a weak formulation to impose boundary conditions.

In case 3, we consider the simple case-1 pipeline equipped with high-speed pressure regulator and shut-off valves, keeping all the remaining conditions unchanged. In this case, the over-pressure due to mass accumulation is small when compared with the wave-pressure amplitude, Fig. 3. Results for case 4 show that inserting a small expansion chamber in the pipeline, with length $L_2 = 10$ m and diameter $D_2 = 0.949$ m, is an effective way of introducing partial reflections of the pressure wave and decreasing the maximum pressure value within the system, Fig. 3.

Cases 5 and 6 refer to a longer pipeline in comparison with the length of the pipelines considered in earlier examples. In case 5 we consider the simultaneous closure of the turbine shut-off valves of the three turbo-generator sets. Under theses conditions, the results of the numerical simulation, plotted in Fig. 4, show that the volume of the pipeline is now sufficiently large for

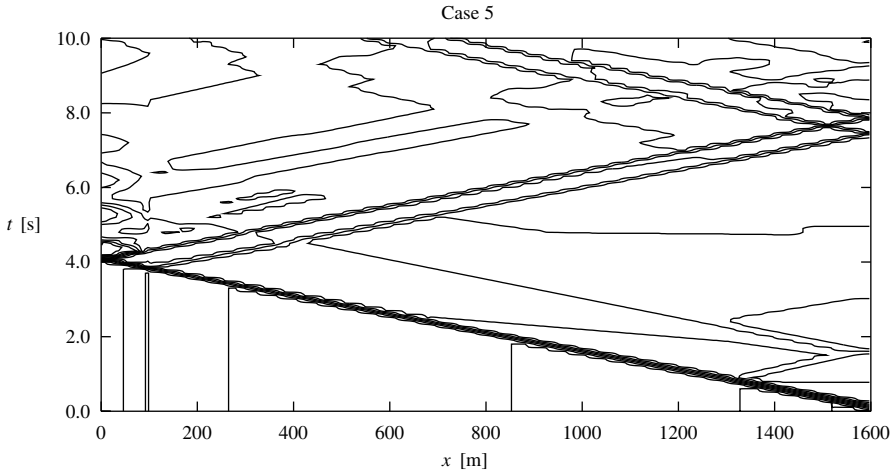

Fig. 5. Isolines of pressure for the first 10 s after the turbine shut-off valves closure, as function of the pipeline position, for case 5.

the pressure increase due to mass accumulation to be similar to the wave pressure amplitude. The pressure irregularities observed in the pressure evolution are due to the partial reflection of the pressure wave at the zone of transition between pipeline elements of different cross-sectional areas, as can be seen in the isolines of Fig. 5. In case 6 we consider the simultaneous partial closure of the protective turbine valves to provide a reduction of the flow rate to 2/3 of its initial value, keeping the remaining conditions unchanged. In this case, the results from the numerical simulation show that the new equilibrium flow conditions are rapidly achieved, with relatively weak pressure fluctuations, Fig. 4.

6. Conclusions

The dynamic behaviour of high-pressure natural-gas flow in pipelines was computed with third-order accuracy in space and time, by solving the one-dimensional time-dependent compressible-flow equations with the Runge–Kutta discontinuous Galerkin method.

The boundary conditions were imposed using a new weak formulation based on the characteristic variables. This formulation allowed the prediction of accurate results for both steady and transient flow conditions. The extension of the boundary conditions to two- and three-dimensional flows is straightforward by considering the eigenvectors associated with the perturbations propagated in the direction normal to the boundary.

The occurrence of pressure oscillations in natural-gas pipelines was studied as a result of the compression wave originated by the rapid closure of downstream shut-off valves. The effect of the partial reflection of pressure waves was also analyzed in the transition between pipes of different cross-sectional areas. The numerical results show that the value of maximum pressure in the pipeline is mainly dependent on the dynamic characteristics of the pressure regulator and the shut-off valves, the pipeline volume, and on the change in the duct cross-sectional area.

References

Abgrall, R., Sonar, T., Friedrich, O., Billet, G., 1999. High order approximations for compressible fluid dynamics on unstructured and cartesian meshes. In: Barth, T.J., Deconinck, H. (Eds.), High-order Methods for Computational Physics, Lecture Notes in Computer Science and Engineering, vol. 9. Springer, Berlin, pp. 1–68.

Barth, T., 1999. Simplified discontinuous Galerkin methods for systems of conservation laws with convex extension. NASA Technical Report NAS-99-009.

Barth, T., Charrier, P., 2001. Energy stable flux formulas for the discontinuous Galerkin discretization of first-order non-linear conservation laws. NASA Technical Report NAS-01-001.

Cockburn, B., 1999. Discontinuous Galerkin method. In: Barth, T.J., Deconinck, H. (Eds.), High-order Methods for Computational Physics, Lecture Notes in Computer Science and Engineering, vol. 9. Springer, Berlin, pp. 69–224.

Cockburn, B., Shu, C.W., 1989. TVB Runge–Kutta local projection discontinuous Galerkin finite element method for conservation laws II: General framework. Math. Comput. (52), 545–581.

Greyvenstein, G.P., 2002. An implicit method for the analysis of transient flows in pipe networks. Int. J. Numer. Methods Eng. (53), 1127–1143.

Hirsch, C., 1990. Numerical Computation of Internal and External Flows, vol. 2. John Wiley & Sons, New York.

Ibraheem, S.O., Adewumi, M.A., 1999. On total variation diminishing schemes for pressure transients. J. Energy Res. Tech.-Trans. ASME 121 (2), 122–130.

Kessal, M., 2000. Simplified numerical simulation of transients in gas networks. Chem. Eng. Res. Design 78 (A6), 925–931.

Osiadacz, A.J., Chaczykowski, M., 2001. Comparison of isothermal and non-isothermal pipeline gas flow models. Chem. Eng. J. 81 (1–3), 41–51.

Rao, C.V.K., Eswaran, K., 1993. On the analysis of the pressure transients in pipelines carrying compressible fluids. Int. J. Pres. Ves. Pip. 56 (1), 107–129.

Shu, C.W., 1999. High order ENO and WENO schemes. In: Barth, T.J., Deconinck, H. (Eds.), High-order Methods for Computational Physics, Lecture Notes in Computer Science and Engineering, vol. 9. Springer, Berlin, pp. 439–582.

Thorley, A.R.D., Tiley, C.H., 1987. Unsteady and transient flow of compressible fluids in pipelines—a review of theoretical and some experimental studies. Int. J. Heat Fluid Flow 8 (1), 3–15.

Zhou, J.Y., Adewumi, M.A., 2000. Simulation of transients in natural gas pipelines using hybrid TVD schemes. Int. J. Numer. Methods Fluids 32 (4), 407–437.